Techno-economic assessment of blue and green ammonia as energy carriers in a low-carbon future

Carlos Arnaiz del Pozo [a], Schalk Cloete [b],*

[a] *Universidad Politécnica de Madrid, Madrid, Spain*
[b] *Flow Technology Group, SINTEF Industry, Trondheim, Norway*

ABSTRACT

Ammonia is an industrial chemical and the basic building block for the fertilizer industry. Lately, attention has shifted towards using ammonia as a carbon-free energy vector, due to the ease of transportation and storage in liquid state at $-33\,°C$ and atmospheric pressure. This study evaluates the prospects of blue and green ammonia as future energy carriers; specifically, the gas switching reforming (GSR) concept for H_2 and N_2 co-production from natural gas with inherent CO_2 capture (blue), and H_2 generation through an optimized value chain of wind and solar power, electrolysers, cryogenic N_2 supply, and various options for energy storage (green). These longer-term concepts are benchmarked against conventional technologies integrating CO_2 capture: the Kellogg Braun & Root (KBR) Purifier process and the Linde Ammonia Concept (LAC). All modelled plants utilize the same ammonia synthesis loop for a consistent comparison. A cash flow analysis showed that the GSR concept achieved an attractive levelized cost of ammonia (LCOA) of 332.1 €/ton relative to 385.1–385.9 €/ton for the conventional plants at European energy prices (6.5 €/GJ natural gas and 60 €/MWh electricity). Optimal technology integration for green ammonia using technology costs representative of 2050 was considerably more expensive: 484.7–772.1 €/ton when varying the location from Saudi Arabia to Germany. Furthermore, the LCOA of the GSR technology drops to 192.7 €/ton when benefitting from low Saudi Arabian energy costs (2 €/GJ natural gas and 40 €/MWh electricity). This cost difference between green and blue ammonia remained robust in sensitivity analyses, where input energy cost (natural gas or wind/solar power) was the most influential parameter. Given its low production costs and the techno-economic feasibility of international ammonia trade, advanced blue ammonia production from GSR offers an attractive pathway for natural gas exporting regions to contribute to global decarbonization.

1. Introduction

The widespread resolution to decarbonize the world economy (IEA. [1]) has directed increasing attention towards the development of low-carbon energy vectors. Recently, H_2 has received a notable interest (IEA. [2,3]) as it constitutes an energy carrier which can displace carbon-intensive fuels in various sectors while providing an effective solution for variable renewable electricity integration (Cloete et al. [4]). Despite numerous policies supporting the development of the H_2 economy (Kovac et al. [5]), its low volumetric energy density creates substantial techno-economic challenges in transportation, storage and distribution, despite ongoing progress (Nazir et al. [6], Wang et al. [7]). Thus, alternatives such as ammonia have been identified to overcome the inherent difficulties of handling H_2, since the former has a boiling point

of around $-33.4\,°C$ and can be stored cheaply at ambient pressure in large quantities (Bartels et al. [8]), with a well-developed pre-existing infrastructure for transportation (Elishav et al. [9]). In contrast, H_2 liquifies at $-252.8\,°C$, undergoing an ortho-para exothermic conversion in the cooling process (Hande et al. [10]), which requires very large energy inputs and expensive and complex equipment (Hammad et al. [11]), making this energy storage route less feasible at a large scale. On the other hand, although ammonia is actually used primarily for nitrogen-based fertilizer production (Jeonghoon et al. [12]), it shows good potential for applications as fuel in thermal power generation (Ezzat et al. [13]) and transport (Hansson et al. [14]) sectors, and it can be reconverted to H_2 through thermolysis at the point of use (Cechetto et al. [15]). Power-to-ammonia-to-power small-scale technologies have been evaluated for islanded energy storage (Rouwenhorst et al [16]).

Given the potential of ammonia to help accelerate the global energy

---

Nomenclature

Acronyms

ACF	Annualized cash flow
ASME	American Society of Mechanical Engineers
ATR	Autothermal reformer
CCS	Carbon capture and storage
CPU	Cryogenic purification unit
EoS	Equation of state
IEA	International energy agency
IRENA	International renewable energy agency
FTR	Fired tubular reformer
GSR	Gas switching reforming
HB	Haber-Bosch
HP	High pressure
HTS	High temperature shift
IP	Intermediate pressure
KBR	Kellogg, Braun & Root
LAC	Linde ammonia concept
LCOA	Levelized cost of ammonia
LCOP	Levelized cost of product
LHV	Lower heating value
LNG	Liquified natural gas
LP	Low pressure
LTS	Low temperature shift
MDEA	Methyl-diethanolamine
NG	Natural gas

NPV	Net present value
PEM	Polymer electrolyte membrane
PSA	Pressure swing adsorption
PR	Peng Robinson
RKS	Redlich Kwong Soave
SEA	Standardized economic assessment
SC	Specific consumption
S/C	Steam to carbon
SMR	Steam methane reforming
T&S	Transport & storage
WGS	Water gas shift

List of Symbols

C_{CO_2}	Capture rate (%)
f	Fugacity (bar)
i	Discount rate (-)
K_{eq}	Equilibrium constant (-)
E_{CO_2}	Specific emissions (ton/ton)
E_{ab}	Backward reaction activation energy (kJ/mol)
k_{0b}	Backward reaction pre-exponential factor (-)
$\dot{m}$	Flow rate (kg/s)
r	Species reaction rate (kmol/m^3·h)
t	Time (s)
$\dot{W}$	Work (kW)
α	Kinetic correlation parameter (-)
η	Efficiency (%)
ϕ	Capacity factor (%)

transition, interest is growing in producing it from fossil fuels with CO_2 capture (blue NH_3), and from renewable electrolytic hydrogen (green NH_3). Regarding blue NH_3 production, new synthesis pathways with a minimal CO_2 emissions have been proposed recently (Cloete et al. [17], Pereira et al. [18], Martínez et al. [19]). The primary lever for improving the performance of blue NH_3 plants is enhancing the fuel conversion efficiency to H_2. One promising route to accomplish this goal is chemical looping reforming (Rydén et al. [20]), a variant of chemical looping combustion (Ishida et al. [21]), to efficiently supply heat to the endothermic steam methane reforming reaction while avoiding CO_2 emissions. However, operation of pressurized interconnected fluidized beds with solids circulation is challenging and progress in this direction has been slow (Mattisson et al. [22]). Zaabout et al. [23] proposed an alternative operation where the oxygen carrier remains in a single fluidized vessel while it is alternatively exposed to oxidizing and reducing streams by means of gas switching valves. Recent studies evaluated the performance of dynamically operated packed bed reactors for H_2 production (Spallina et al. [24]) and their integration in ammonia production process (Pereira et al. [18]). Through operation in fluidization mode, using the gas switching reforming (GSR) concept (Wassie et al. [25]), challenges related to packed bed reactor heat management are avoided, but undesired mixing of the outlet streams from each reactor step occurs, reducing both the CO_2 capture performance and the purity of the CO_2 product.

Similarly, the prospects of green NH_3 production (Zhang et al. [26], Sánchez et al. [27], Ozturk et al. [28]) depend primarily on the cost at which a sufficiently steady stream of electrolytic hydrogen can be supplied to the ammonia synthesis loop. Given the rapidly falling costs of wind and solar power (IRENA [29]) and electrolysers (IRENA [30]), this pathway is also attracting increasing research and demonstration interest (IEA [2]). Nonetheless, recent studies for solar driven ammonia achieve levelized costs of 718 $/ton (Osman et al. [31]), highlighting that this production pathway still requires considerable efficiency enhancements and capital cost reductions to make commercial sense for base chemical production (Wang et al. [32]). On the other hand,

offshore wind power to ammonia requires substantial power grid back-up for successful deployment (Morgan et al. [33]), resulting in potential carbon emissions associated to those electricity imports. Finally, green ammonia processes with exceptional wind and solar resources in Patagonia and flexible synthesis loop design can reach levelized costs as low as 483 $/ton (Armijo et al. [34]).

In the present study, the techno-economic performance of blue and green NH_3 plants is assessed using a consistent methodology. Two blue NH_3 process configurations currently in commercial operation are evaluated as reference plants, whereas advanced blue NH_3 production using the GSR concept and green NH_3 production using low-cost wind, solar, and electrolyser technologies expected around mid-century are evaluated as longer-term deployment options for large-scale NH_3 production as a carbon-free energy carrier.

1.1. Technology overview

The first reference plant is the Kellogg, Braun & Root (KBR) purifier process (Gosnell [35]), schematically represented in Fig. 1 A). It features a fired tubular reformer (FTR) and an autothermal reformer (ATR) where the required N_2 is supplied through combustion of syngas with air. A two-step adiabatic water gas shift (WGS) train maximizes H_2 production, followed by a CO_2 removal step, which produces a pure CO_2 stream for utilization or storage. The subsequent cryogenic purification unit adjusts the make-up syngas composition optimally and removes inert species that would otherwise accumulate in the loop.

The second reference plant is the Linde Ammonia Concept (LAC) (Pattabathula et al. [36], Linde-engineering [37]), briefly depicted in Fig. 1 B). Contrary to the KBR process, it employs only a primary reformer, while the N_2 for the synthesis reaction is generated in a dedicated cryogenic generation unit. The syngas from the reformer undergoes an isothermal shift and after CO_2 removal through absorption it is purified in a Pressure Swing Adsorption (PSA) unit. Thus, the fresh syngas for the ammonia loop in the LAC concept is highly purified, and the purge requirements are substantially reduced.
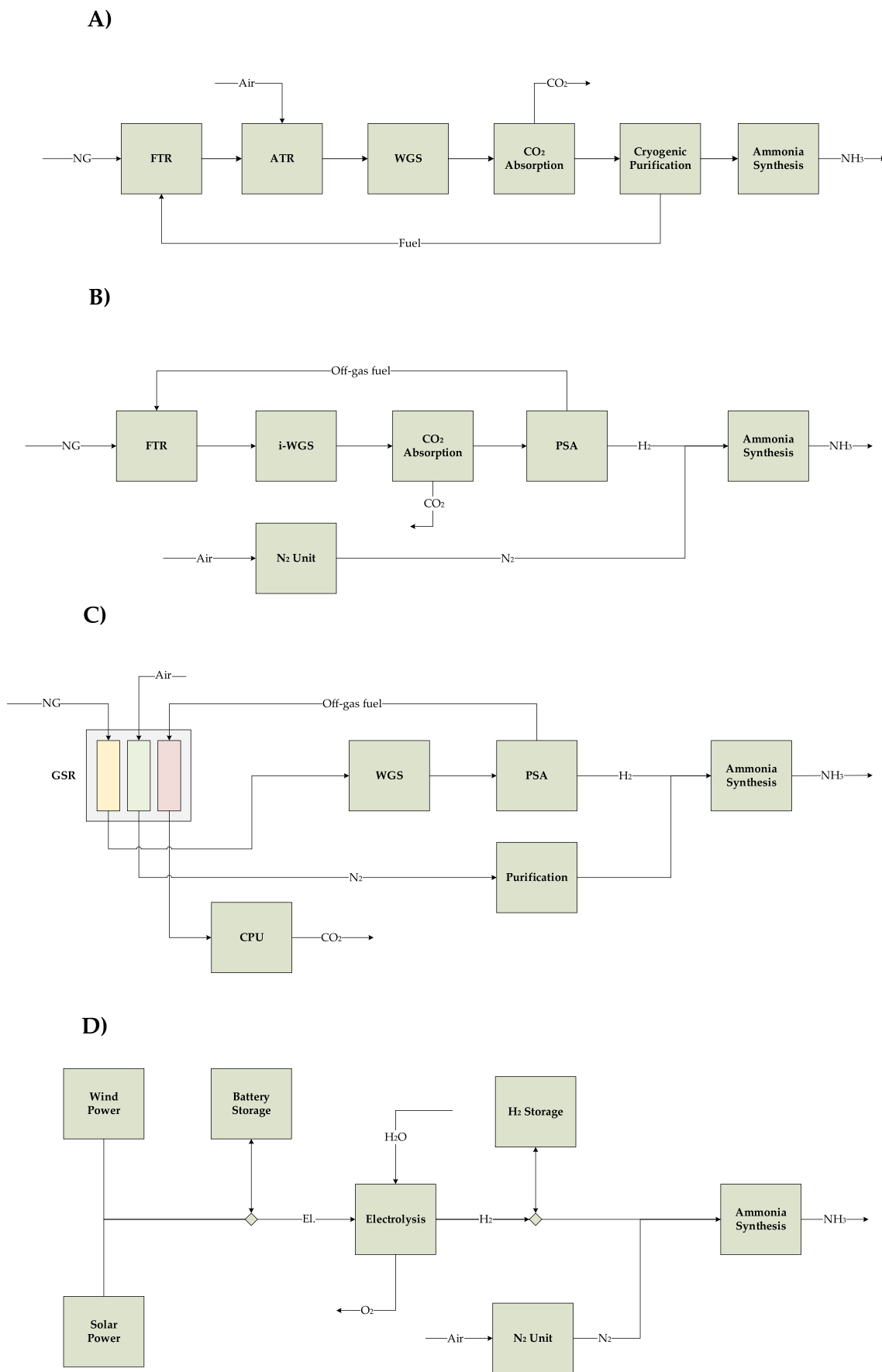
A)

B)

C)

D)

Fig. 1. Block flow diagrams of different ammonia production technologies: A) KBR B) LAC C) GSR and D) Green-NH_3. (For interpretation of the references to colour in this figure legend, the reader is referred to the web version of this article.)

The GSR-NH$_3$ process is investigated as a longer-term blue NH$_3$ pathway. In this scheme, represented in Fig. 1 C), a cluster of dynamically operated fluidized beds delivers syngas from the reforming step, which undergoes a WGS conversion to enhance H$_2$ yield, to a PSA unit. The off-gas stream is compressed and recycled to the GSR cluster reduction step, providing the heat of reaction required in the reforming step. The pressurized N$_2$ stream from the oxidation step outlet is purified, mixed with H$_2$ from the PSA and fed to the synthesis loop.

Finally, the green NH$_3$ route, briefly depicted in Fig. 1 D), involves electrolytic hydrogen production and cryogenic N$_2$ generation to feed the ammonia synthesis loop. An important feature of this plant is the requirement for energy storage to account for the renewable power intermittency (Nayak-Luke et al. [38]). Energy can be stored as electricity, hydrogen, or ammonia.

In the following sections, each of the plants is described in greater detail. The ammonia synthesis loop (with refrigeration unit) common to all plants is then presented. Subsequently, the key performance parameters in terms of energy and CO$_2$ emissions are defined, while the economic framework for the evaluation is discussed. Next, the results for all the configurations are provided, including a sensitivity analysis to the key economic assumptions. Finally, the main conclusions of the work are discussed.

2. Methodology

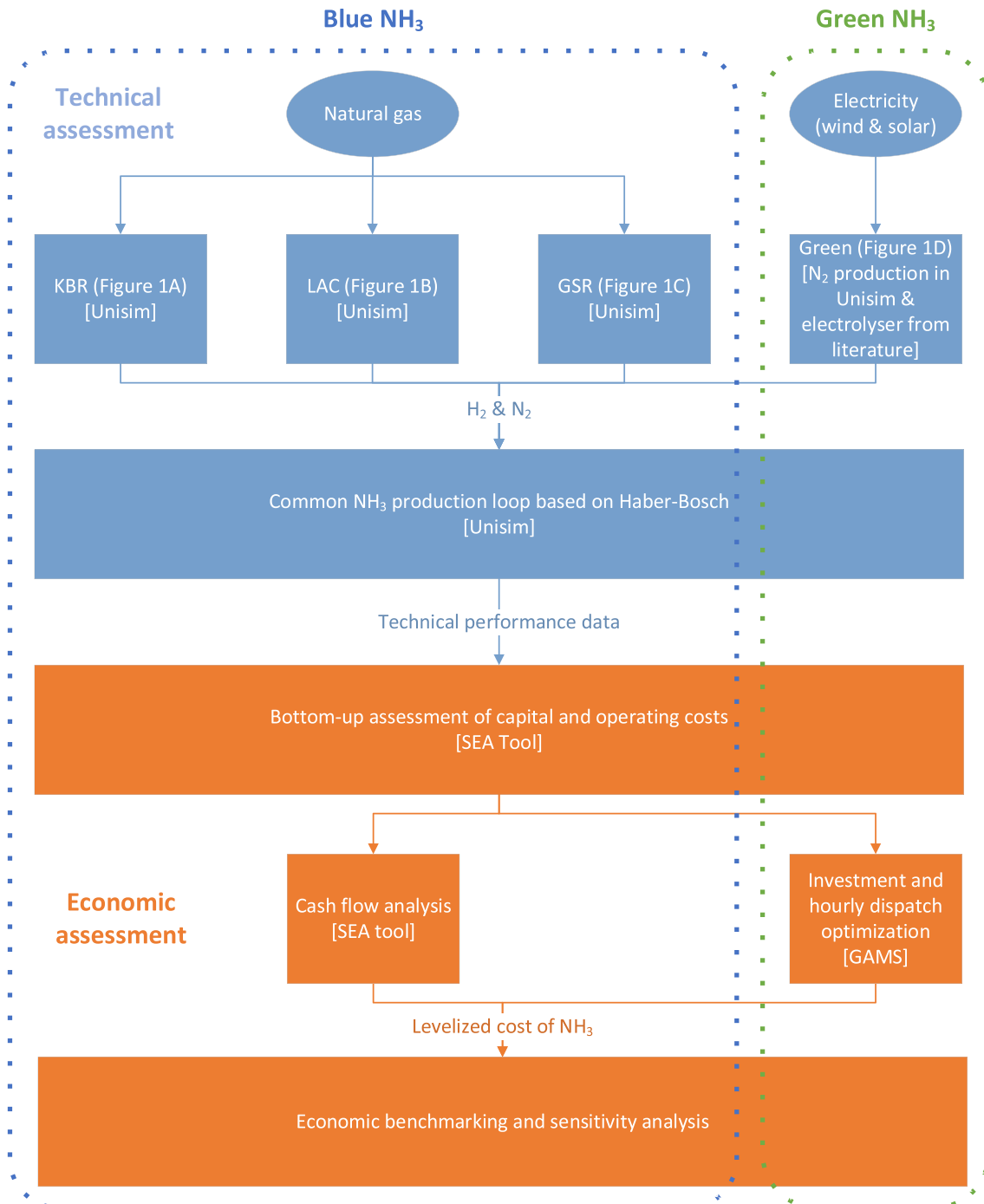In this section, a more detailed description of the four ammonia

Fig. 2. Graphical representation of the methodology employed in this work.

plants is provided, with emphasis on their characteristic features, followed by a separate section on the ammonia synthesis loop employed for all configurations. As shown in Fig. 2, blue and green NH_3 plants are modelled using slightly different methodologies. The blue plants could be assessed using process modelling followed by an economic assessment assuming steady-state operation. The green NH_3 plant, on the other hand, required dedicated optimization of investment and hourly dispatch of all the technologies illustrated in Fig. 1D to transform fluctuating wind and solar power production to a steady NH_3 output in the least-cost manner.

The models were built in Unisim Design R481, using the Peng-Robinson (PR) equation of state (EoS) for property estimation of the main process streams. For the steam cycle ASME steam cycles were used. For the MDEA absorption units proprietary DRB Amine: Kent-Eisenberg package was selected to estimate absorption performance. The synthesis loop was modelled using the Redlich-Kwong Soave (RKS) EoS, as recommended by Flórez-Orrego et al. [39], which provided better approximations to the synthesis loop performance shown in this study. The GSR dynamic model was modelled in Scilab, with an in-house thermodynamic package Patitug, and was connected to the stationary simulator with a CAPE-OPEN unit operation. Relative energy balance errors between the two simulation platforms resulted below 0.1%. Finally, the plant performance indicators from an energy, environmental and economic perspective are defined, providing the adequate criteria to evaluate each of the concepts. Plant configurations are presented in detail in the supplementary file attached to this manuscript, together with corresponding stream summaries, main modelling and equipment performance assumptions, as well as the framework for green ammonia cost estimation.

2.1. Reference NH_3 plants

In this work, two well established ammonia production technologies are studied as reference plants: the Kellogg, Braun & Root (KBR) Purifier process and the Linde Ammonia Concept (LAC), which employ conventional steam methane reforming for H_2 generation, and differ in the method by which the reactants are delivered to the synthesis loop. Given that the novel GSR-NH_3 plant would be potentially deployed when CO_2 taxes will become significant, the reference plant models developed in this study also incorporate CCS. In unabated ammonia production plants, CO_2 from the MDEA stripper column is directly vented to the atmosphere, and CCS implementation only requires pressurization of this stream with an intercooled compressor and a supercritical pump. When available, carbon free fuel is employed in the reformer and/or auxiliary units of these plants.

2.1.1. KBR Purifier NH_3 process

Ammonia plants consist of H_2 generation units which feature desulphurization and pre-reforming steps followed by a fired tubular reformer (FTR), where heat for endothermic natural gas reforming is delivered externally by combustion of fuel with air close to its stoichiometric ratio. The steam to carbon ratio is set to 2.7, to avoid carbon deposition in the nickel catalyst bed within the reformer tubes. In the KBR Purifier ammonia process, more than the stoichiometric amount of N_2 (for ammonia synthesis) is introduced with air in the subsequent autothermal reformer (ATR), achieving a methane fraction of around 3% on a dry basis at the outlet. The air stream is compressed by means of a gas turbine, whose hot exhaust outlet is fed to the furnace of the primary reformer, maximizing heat integration. Since air is introduced in excess to the ATR, reforming duty is shifted towards the secondary reformer, and the temperature outlet of the FTR is only at around 700 °C.

After heat recovery from the syngas stream outlet of the ATR, raising high pressure (HP) steam, a downstream water gas shift train maximizes H_2 production. Heat from the exothermic WGS reaction is used to raise more steam and economize water. The heat recovery section is optimally integrated with the ammonia loop heat exchangers, and the superheated

steam, at 550 °C and 110 bar, is expanded in the stream turbine to produce power. Two steam extractions from the turbine are present: at an intermediate pressure (IP) at 34 bar to reach the S/C in the reformer inlet, and at a low pressure (LP) of 3 bar to supply heat for amine regeneration in the stripper reboiler of the absorption unit. Once the syngas is cooled to ambient temperature and condensed water is knocked out, 99% of the CO_2 is removed in an MDEA absorption process; the stripper column tops (CO_2) is further compressed in a four-stage intercooled compressor and pumped to 150 bar delivery pressure. The syngas is then routed to a methanation reactor which converts remaining CO and CO_2 to methane, reaching ppm levels of these harmful components in the catalyst beds. Prior to compression and addition of syngas to the loop, the reactor effluent is routed to a cryogenic purification unit, where the H_2/N_2 ratio is adjusted to the stoichiometry of the synthesis reaction while at the same time methane and Argon impurities are reduced to below 0.3%mol. The waste stream containing most of the methane, excess N_2 and some H_2 is used as fuel for the primary reformer and the ATR air compressor gas turbine.

The reactor effluent is then compressed to 150 bar and mixed with the recycle from the NH_3 synthesis loop, which is described in greater detail in a subsequent section. The purge stream from the loop allows to extract argon and methane which was not removed through the cryogenic process. The light species obtained from NH_3 product liquefaction are mixed with the purge and delivered as carbon free fuel for the gas turbine and primary reformer, together with the cryogenic waste stream. Proprietary KBR Purifier process features a synthesis loop employing a Ruthenium catalyst (Bingyu et al. [40]), more active than conventional iron-based catalysts, which enables lower synthesis loop operating pressures and presents a substantially higher cost. However, in this study, the same kinetics for an iron-based catalyst (Dyson et al. [41]) and synthesis loop topology is considered for all plants for a comprehensive comparison.

2.1.2. LAC Linde NH_3 concept

In contrast to the traditional KBR scheme, the LAC plant does not feature an ATR to supply N_2 for the synthesis reaction. Instead, H_2 production consists only of a primary reformer (FTR) operating with a S/C ratio of 2.7 followed by an isothermal shift, in which intermediate pressure (IP) steam is generated and supplied directly to the natural gas feedstock to the reformer. After cooling down and knock out of water from the shifted syngas stream, 99% of the CO_2 is removed in the absorption column with MDEA, after which the H_2 rich syngas is routed to a PSA unit, obtaining a highly pure H_2 stream for the synthesis loop, with a high recovery ratio. The PSA off-gas, containing unconverted methane, CO and some H_2 is used as fuel in the primary reformer.

N_2 for the reaction is supplied at a stoichiometric ratio through an N_2 generation unit. The scope of this unit can vary depending on whether an application for pure O_2 production is available, in which case a full scope air separation unit (ASU) is integrated to the ammonia plant. Alternatively, if only N_2 is required, the cryogenic unit can be greatly simplified. This is the approach taken in the current design, where the scope comprises a single air compression stage and distillation column, retrieving around 60% of the N_2 from the feed with a purity above 99.9%mol. The remaining enriched air (37%mol) is used in the primary reformer furnace.

Given the high purity of the H_2 and N_2 streams comprising the make-up syngas to the synthesis loop, only a very small purge fraction is required. This small purge and the off-gas from the PSA unit are sufficient to satisfy the primary reformer duty demand. The heat recovery section of the syngas cooling from the reformer and the NH_3 synthesis reactor intercoolers is highly integrated, delivering HP steam at 550 °C and 110 bar to a steam power cycle. Similarly to the KBR design, two steam extractions from the steam turbine are present to reach the S/C ratio in the feed and for amine regeneration at IP a LP levels, respectively. Due to the relatively large power input required for N_2 separation and compression, and additional CO_2 pressurization, the LAC concept

presents and electricity deficit, which must be satisfied with power imports to the plant, which are assumed in this study as a variable operating cost.

2.2. Future NH$_3$ plants

The longer-term NH$_3$ production plants considered in this work consist of a blue NH$_3$ plant based the GSR concept and a green NH$_3$ plant using electrolytic hydrogen from wind and solar power, as discussed in this section.

2.2.1. GSR-NH$_3$ plant

As described earlier, the integration of GSR with a PSA unit is an effective pathway to supply the reactants to the ammonia synthesis loop. The GSR island design features the enhancement strategies described in earlier works (Nazir et al. [42,43]), including a two-phase exchanger to maximize condensation enthalpy recovery from the reduction step outlet stream. The S/C is specified to achieve isothermal operation in the GSR reactor cycle. the maximum reactor temperature assumed in this study was 1000 °C (100 °C lower than earlier studies) to minimize the technical challenges from oxygen carrier degradation and downstream switching valves. Details about the dynamic GSR reactor model integrated with the process simulation are provided in the Supplementary Material.

The GSR-NH$_3$ plant presents a high degree of heat integration in the GSR reformer island: due to the high-pressure operation between the inlet and outlet streams of the GSR, closer temperature approaches due to higher heat transfer rates can be reached compared to heat recovery from atmospheric pressure flue gases in conventional reforming. Special provisions in heat exchanger materials (Guo et al. [44]) can be taken to avoid potential issues because of metal dusting (Holland et al. [45]), and nickel alloys are assumed as heat exchanger materials in the economic assessment. The hot N$_2$ product from the GSR oxidation step is used to preheat the inlet air in a recuperator and subsequently to superheat steam from the heat recovery section of the NH$_3$ synthesis loop. The stoichiometric portion of N$_2$ required for NH$_3$ synthesis is split, and the remainder is expanded in a small turbine to retrieve some electrical power. The pressurized N$_2$ stream for synthesis is cooled to ambient and purified through adsorption, removing moisture and CO$_2$ (originating from undesired mixing in the GSR) to ppm levels. Established and available technology based on adsorption (Rege et al. [46]) can be effectively used to accomplish this purity requirement [47]. Alternatively, a methanation step can be employed as suggested by Pereira et al. [18], but this is detrimental for the H$_2$ efficiency, while further increasing the impurities fed to the synthesis loop (in the form of methane).

After cooling down to 300 °C the syngas stream from the GSR reforming step undergoes a two-step adiabatic shift and, after water knock out, it is boosted to 68 bar to maximize recovery of H$_2$ in the subsequent PSA unit, which is modelled with a recovery correlation derived by Nazir et al. [43]. Enhanced H$_2$ recovery in the PSA minimizes the heating value remaining in the off-gas fuel, thereby limiting the required S/C ratio in the natural gas feed to attain isothermal cycle operation. The purified N$_2$ stream is also boosted in a small compressor and then mixed with the PSA H$_2$ product, after which the stream is compressed to the NH$_3$ synthesis loop pressure of 150 bar. A small fraction of inert Ar from the air stream is present in this make-up syngas stream, with a concentration of approximately 0.3%mol, similarly to the purities attained with the cryogenic purifier of the KBR process. The PSA off-gas is recompressed to the GSR reactor pressure level and heated in a recuperator with the CO$_2$-rich outlet stream from the GSR reduction step before being fed as fuel to the GSR reduction step. After the recuperator, the reduction outlet is routed to the two-phase exchanger for maximum recovery of the condensation enthalpy, and then cooled down to ambient, knocking out condensed water. At this point, the CO$_2$ purity is somewhat below the required specifications for transport and storage

(Kolster [48]), therefore, a cryogenic purification unit is necessary (Campanari et al. [49]) to comply with the regulations.

The fresh make up gas is fed to the NH$_3$ synthesis loop (H$_2$, N$_2$ and some Argon) after a booster compression stage to 150 bar. The purge from the loop is recycled to the PSA unit, to retrieve H$_2$ as a reactant and remove impurities which are then incorporated in the PSA off-gas fuel to the GSR reduction step, and finally removed (partially) with the CPU. The purge fraction is optimized such that the loop recirculation and booster compressor yield the minimum auxiliary power demand. Heat produced in the WGS reaction, GSR oxidation outlet and NH$_3$ synthesis loop is used to generate HP steam for the power cycle, which features an IP reheating step to avoid excess condensation in the LP stage turbine outlet. Given the large power consumption of the air and PSA-off gas recycle compressors, the GSR-NH$_3$ will present the largest electricity demand of the blue ammonia plants, although this is compensated by a much higher H$_2$ production efficiency.

2.2.2. Green NH$_3$ plant

The green ammonia plant features a low-temperature electrolyser (alkaline or PEM) that produces H$_2$ at 30 bar from water splitting using renewable electricity at a projected 2050 efficiency of 70% (LHV) derived from European targets [50]. N$_2$ is supplied similarly to the LAC plant, with a dedicated cryogenic unit, resulting in minimal capital cost. The synthesis loop (including refrigeration and storage) is identical to the other models, as discussed in the next section. The smaller power cycle for the green ammonia plant only generates steam at 110 bar from the NH$_3$ synthesis loop heat exchangers, with a maximum superheat temperature determined by the 1st reactor bed outlet. An intermediate reheat to 400 °C is needed to avoid excess condensation in the low-pressure stage outlet.

The simulated processes represent the "Ammonia Synthesis" and "N$_2$ Unit" blocks in Fig. 1 D), while the remaining blocks are added in the system-level optimization tool detailed in the Supplementary Material. The system model optimizes investment and hourly dispatch of each technology in Fig. 1 D) for one representative year to achieve the minimum achievable ammonia production cost using wind and solar resources from three regions: Northern Germany, Southern Spain, and Saudi Arabia.

2.3. NH$_3$ synthesis loop

The Haber-Bosch (HB) synthesis loop for ammonia production is the same for all models, including the reference plants, and is briefly depicted in Fig. 3. Such a baseline enables a consistent comparison between the different H$_2$ generation methods of each of the process concepts. This section of the plant was modelled based on the study performed by Flórez-Orrego et al. [39] for large scale ammonia production, consisting of a three-bed reactor design with heat recuperation between the first bed inlet feed and the outlet, and steam generation after the second and third beds. The heat recovery exchangers consist of steam superheaters, evaporators and an economizer after the last bed, when the heat recovery section of the reformer island cannot supply enough hot water. Cooling of the effluent after each reactor bed maximizes the conversion per pass (as the exothermic nature of the reaction limits equilibrium), reducing the recycle of reactants and improving the yield of the available reactor volume. The inlet temperature to each bed must be selected such that it is sufficiently high for the reaction to proceed at a fast rate, but not to the point where conversion is hindered by equilibrium. Flórez-Orrego et al. [39] carried out an exergy optimization by tuning the inlet bed temperature of each bed for a specific fresh syngas composition. In this study, all models assume an inlet temperature of 350 °C, 400 °C and 400 °C for 1st, 2nd and 3rd bed respectively. The reactor volume was specified assuming a nominal production of 3000 tpd, within the capacity range of modern large-scale ammonia plants. The rate of reaction r_{N_2} is provided in Eq. (2) (Dyson et al. [41]), as a function of the fugacities f_k of the species involved; the parameters
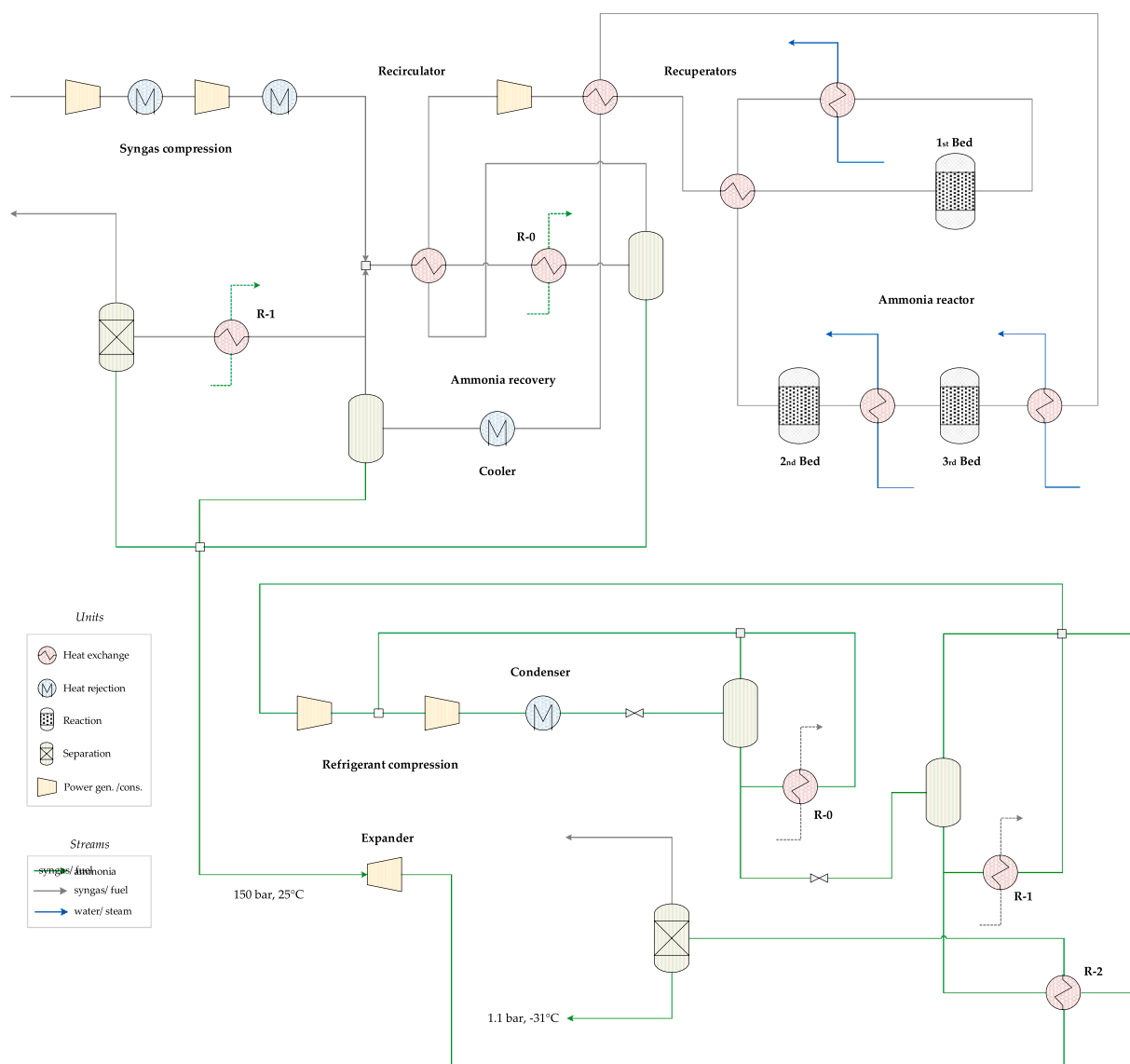
Fig. 3. Ammonia synthesis loop with product refrigeration common to all models.

for the backward kinetic constant k_b are presented in Table 1, while K_{eq} corresponds to the equilibrium constant of the reaction in Eq. (1). The beds were simulated in Unisim as a plug flow reactor using a large ratio between reactor diameter and catalyst particle, similarly to [39], with the bed properties summarized in Table 2.

$$N_2 + 3H_2 \leftrightarrow 2NH_3 \tag{1}$$

$$-r_{N_2} = k_b \left[K_{eq} f_{N_2} \left(\frac{f_{H_2}^3}{f_{NH_3}^2} \right)^\alpha - \left(\frac{f_{NH_3}^2}{f_{H_2}^3} \right)^{1-\alpha} \right] \left[\frac{kmol}{m_{cat}^3 \hat{A} \cdot h} \right] \tag{2}$$

The discharge pressure from the make-up syngas compressors was set to 150 bar. After steam generation downstream the third bed, the reactants in the recycle loop are cooled down with the discharge outlet of

Table 1
Kinetic parameters of the backward reaction [39].

k_{0b}	2.57×10^{14}
E_{ab}	163500 (kJ/mol)
α	0.55

Table 2
Reactor bed properties [39].

Property	Value	Units
Bed voidage	0.46	–
Catalyst density	2300	kg/m^3
Particle diameter	3	mm
Total bed volume	294.3	m^3

the recirculation compressor, to maximize recovery of the enthalpy of reaction. It is further cooled to ambient, condensing a large fraction of the product ammonia. From the gaseous stream a small split is withdrawn (purge) to avoid accumulation of inerts in the loop, and the main portion is subsequently mixed with the compressed make-up syngas. This stream is subsequently cooled down to -20 °C in R-0 to further recover the reaction product [19]. Mixing the make-up prior to this condensation step is desirable to eliminate traces of carbonaceous components from entering the reactor, as such components will preferentially dissolve in the liquid ammonia. A small refrigerant exchanger R-1 is also included in the purge stream to avoid NH$_3$ losses. The condensed ammonia is expanded in a flashing liquid turbine to close to atmospheric pressure, and the vaporized fraction (around 10%) is

liquefied in R-2. As a refrigerant, ammonia itself is employed. Given the high volatility of the small fraction of species other than NH_3 in the stream it is assumed that they are entirely retrieved as fuel gas in a subsequent purification step, reaching high grade ammonia purities (>99.99% mol.) in the final product [51], which is stored in liquid state at approximately −31 °C and 1.1 bar.

For green NH_3 simulations, added costs related to flexible synthesis loop operation must also be estimated. In this work, these costs are represented by efficiency losses associated with part-load operation, represented as extra energy consumption amounting to 18.8 MW of H_2 and 8.3 MW of electricity (relative to optimal operation) for every 100 MW reduction in NH_3 output. The synthesis loop simulations for part load operation are described in more detail in the Supplementary Material file.

2.4. Plant performance indicators

To provide a holistic perspective of each of the process concepts, several performance metrics need to be defined. In this section such definitions are provided, as well as the underlying assumptions of the economic assessment.

2.4.1. Energy and environmental

A set of common indicators are defined in terms of energy and environmental (CO_2 emissions) performance. The simple efficiency η_{NH_3} is calculated by Eq. (3) attending to the lower heating value input (natural gas) and output (ammonia) from the plant. An intermediate H_2 efficiency η_{H_2} represents the ratio of the H_2 heating value delivered to the synthesis loop with respect to that of the natural gas feed, as defined in Eq. (4). Finally, the net efficiency η_{net} discounts the electricity consumption $\dot{W}_{net}$ from the final product heating value, as shown in , assuming that the energy value of ammonia is similar to that of electricity.

$$\eta_{NH_3} = \frac{\dot{m}_{NH_3} LHV_{NH_3}}{\dot{m}_{NG} LHV_{NG}} \tag{3}$$

$$\eta_{H_2} = \frac{\dot{m}_{H_2} LHV_{H_2}}{\dot{m}_{NG} LHV_{NG}} \tag{4}$$

To account for electricity consumption, an equivalent natural gas consumption is defined that adjusts for the higher value of electricity by dividing electricity consumption by a heat-electricity equivalent η_{el} of 62%, typical of a combined cycle power plant. This equivalent natural gas consumption is then used to calculate an equivalent NH_3 production efficiency (Eq. (6)).

$$\dot{m}_{NG,eq} LHV_{NG} = \dot{m}_{NG} LHV_{NG} + \frac{\dot{W}_{net}}{\eta_{el}} \tag{5}$$

$$\eta_{NH_3,eq} = \frac{\dot{m}_{NH_3} LHV_{NH_3}}{\dot{m}_{NG,eq} LHV_{NG}} \tag{6}$$

Complementary to these efficiencies, the specific consumption SC and equivalent specific consumption SC_{eq} are common performance parameters, and are defined in Eq. (7) and Eq. (8), respectively.

$$SC = \frac{\dot{m}_{NG} LHV_{NG}}{\dot{m}_{NH_3}} \tag{7}$$

$$SC_{eq} = \frac{\dot{m}_{NG,eq} LHV_{NG}}{\dot{m}_{NH_3}} \tag{8}$$

Finally, with regards to CO_2 emissions, the capture ratio C_{CO_2} and specific emissions E_{CO_2} are presented in Eq. (9) and Eq. (10), respectively.

$$C_{CO_2} = \frac{\dot{m}_{CO_2,capt.}}{\dot{m}_{CO_2,emit.} + \dot{m}_{CO_2,capt.}} \tag{9}$$

$$E_{CO_2} = \frac{\dot{m}_{CO_2,emit.}}{\dot{m}_{NH_3}} \tag{10}$$

These definitions, as expressed in Eq. (3) - Eq. (10), apply to the blue ammonia production plants employing a natural gas feedstock. Simpler measures can be used for the green ammonia plant because electricity is the only form of input energy. For green NH_3, η_{H_2} is simply the assumed H_2 production efficiency of 70% (LHV), whereas η_{NH_3} and η_{net} are given in Eq. (11) and Eq. (12), where $\dot{W}_{elec}$ is the power consumption by the electrolysers and $\dot{W}_{HB}$ is additional power consumption in the ammonia production loop. Similarly, the specific consumptions are defined based only on electrolyser electricity consumption and ammonia production (Eq. (13) and Eq. (14)).

$$\eta_{NH_3} = \frac{\dot{m}_{NH_3} LHV_{NH_3}}{\dot{W}_{elec}} \tag{11}$$

$$\eta_{NH_3,eq} = \frac{\dot{m}_{NH_3} LHV_{NH_3}}{\dot{W}_{elec} + \dot{W}_{HB}} \tag{12}$$

$$SC = \frac{\dot{W}_{elec}}{\dot{m}_{NH_3}} \tag{13}$$

$$SC_{eq} = \frac{\dot{W}_{elec} + \dot{W}_{HB}}{\dot{m}_{NH_3}} \tag{14}$$

2.4.2. Economic

The economic evaluation of the ammonia production plants was carried out with the Standardized Economic Assessment (SEA) Tool developed by the authors [52]. A comprehensive user guide of this open-source MS Excel tool is available [53]. Dedicated spreadsheets of the economic evaluations for each process can be found in [54]. Equipment correlations from Turton [55] and capacity cost correlations for different units are used, adjusting the source to the target cost basis of the evaluation, defined in Table 3. Location factors account for the difference between costs of material and labour in different world regions [56].

The main economic assumptions regarding capital cost estimation, fixed (FOM) and variable (VOM) operating costs and cash flow analysis variables are presented in Table 4. The SEA Tool calculates the levelized cost of product (LCOP), as the selling price of ammonia that yields a net present value of zero at the end of the plant lifetime. The NPV is calculated through the summation of the annualized cash flows as shown in Eq. (15) and Eq. (16), where ϕ is the capacity factor and P_{NH_3} is the yearly ammonia production.

$$NPV = \sum_{t=0}^{n} \frac{ACF_t}{(1+i)^t} \tag{15}$$

$$ACF_t = \phi \cdot \left(LCOP \cdot P_{NH_3} - C_{VOM} \right) - C_{Capital} - C_{FOM} \tag{16}$$

Sensitivity analyses to key economic assumptions such as natural gas and electricity prices, CO_2 tax and transport & storage costs, discount rate and capacity factor are carried out to determine the relative influence of these variables for each of the blue NH_3 plants. To facilitate easy interpretation of the results, only one parameter is varied at a time, keeping all parameters at their reference values. In each case, the LCOP is determined to assess the effect of the selected parameter on the final product cost from the process.

The blue ammonia plants are compared to a green ammonia model considering different world regions with different wind and solar

Table 3
Target cost basis details.

Location	Western Europe
Year	2020
Currency	€

Table 4

Economic evaluation assumptions [17,18,57].

Capital estimation methodology		
Bare Erected Cost (BEC)		SEA Tool Estimate
Engineering Procurement and Construction (EPC)		10 % BEC
Process contingency (PC)		0–20 % BEC
Project Contingency (PT)		20 % (BEC + EPC + PC)
Owners Costs (OC)		15 % (BEC + EPC + PT + PC)
Total Overnight Costs (TOC)		BEC + EPC + PC + PT + OC
Operating & maintenance costs		
Fixed		
Maintenance	2.5	%TOC
Insurance	1	%TOC
Labour	60,000	€/y-p
Operators	50–60	Persons
Variable		
Natural gas	6.5	€/GJ
Electricity	60	€/MWh
Oxygen carrier	15	€/kg
Reformer catalyst	15	€/kg
WGS catalyst	16,100	€/m^3
Ammonia reactor catalyst	20	€/kg
CO_2 transport & storage	20	€/ton
CO_2 tax	100	€/ton
Process water	6	€/m^3
Cooling water make-up	0.35	€/m^3
Cash flow analysis assumptions		
1st year capacity factor	65	%
Remaining years	85	%
Discount Rate	8	%
Construction period	4	years
Plant Lifetime	25	years

generation profiles derived from Renewables Ninja (Pfenninger et al. [58]). As shown in Table 5, wind and solar resources are more favourable in Spain and Saudi Arabia than in Germany. Resource availability is also more constant across the year in Saudi Arabia than in Europe. The German solar resource varies especially strongly between summer and winter, although this variation is to some extent offset by a complimentary seasonal variation in the wind resource. In addition, natural gas prices (set according to 2050 projections in the IEA Announced Pledges Scenario [1] where Saudi Arabian prices are assumed equal to US prices) are much lower in Saudi Arabia than in Europe. Saudi Arabian electricity is also assumed to be 33% cheaper than in Europe, whereas CO_2 transport and storage costs are assumed to be cancelled out by enhanced oil and gas recovery from local fields. All other assumptions in Table 4 remain unaltered. Plants constructed in Saudi Arabia may also have lower capital costs than those in Europe, but the latest IRENA numbers [29] show that current utility scale solar PV costs are actually about 35% higher in Saudi Arabia than in Germany and Spain. Hence, capital costs were kept at European levels also for the assessment in Saudi Arabia. Specific sensitivity analyses to wind/solar power production and electrolyser capital cost variations as well as NH_3 production flexibility are presented for the green NH_3 plants as well. The complete optimization is carried out in each sensitivity assessment, allowing the model to adjust the investment in different components for optimal results based on

Table 5

Economic assumptions, modified between regions, for benchmarking against green ammonia.

Item/Location	Germany	Spain	Saudi Arabia
Wind capacity factor (%)	29.5	34.5	32.6
Average wind speed winter/summer (m/s)	7.18/ 6.29	7.69/ 6.64	6.95/6.62
Solar capacity factor (%)	12.4	19.3	21.8
Average direct solar irradiance winter/ summer (W/m^2)	41/155	166/220	238/227
Natural gas price (€/GJ)	6.5	6.5	2
Electricity price (€/MWh)	60	60	40
CO_2 transport and storage (€/ton)	20	20	0

modified cost assumptions.

3. Results

Results will be presented in two sections, first the energy breakdown will be presented for each plant and the key performance indicators in terms of production efficiencies and CO_2 emissions will be shown. Then, the economic study will be presented in detail, evaluating the potential of the plant concepts at different economic parameters from the base values.

3.1. Energy and environmental results

The energy breakdown and performance parameters for the different configurations are provided in Table 6. Notably, the KBR Purifier process accomplishes ammonia production integrating carbon capture with minimal power imports to the plant, resulting in similar values for the specific consumption and equivalent specific consumption. On the other hand, the LAC concept requires substantial electricity imports because of the power required for N_2 separation and compression. Finally, the GSR-NH_3 plant, with energy consuming air and fuel gas compressors, presents the largest electricity demand, but at the same time presents a significantly smaller specific consumption of natural gas, requiring the least heat input to the plant for a fixed ammonia production capacity. When power imports are accounted for in the equivalent specific consumption calculation, the GSR-NH_3 plant remains the most competitive in terms of energy performance, relative to the well-established reference technologies.

Table 6

Energy and environmental results.

Model		KBR	LAC	GSR-NH_3	Green
Item	Units	Value			
Heat Balance					
NG input	MW$_{th}$	989.9	925.3	791.4	–
Electrolyser power	MW$_{el}$	–	–	–	1061.6
H_2 from Reformer/ Electrolyser	MW$_{th}$	799.2	743.1	761.5	743.1
NH_3 output	MW$_{th}$	648.6	646.6	645.6	649.1
Energy					
η_{H_2}	%	80.7	80.3	96.2	70.0
η_{NH_3}	%	65.5	69.9	81.6	61.1
$\eta_{NH_3,eq}$	%	65.4	67.2	71.1	60.1
SC	GJ/ton	28.4	26.6	22.8	30.4
SC$_{eq}$	GJ/ton	28.5	27.7	26.2	31.0
Environmental					
C$_{CO_2}$	%	82.8	76.3	94.4	–
E$_{CO_2}$	ton/ ton	0.28	0.36	0.07	–
Power Breakdown					
Consumers					
Air Blower	MW$_{el}$	1.0	3.4	–	–
Air Compressor	MW$_{el}$	24.1	–	35.3	–
N_2 Unit	MW$_{el}$	0.0	17.6	0.0	17.9
CO_2 Compression	MW$_{el}$	14.4	12.3	3.3	–
CO_2 Pump	MW$_{el}$	0.6	0.5	0.6	–
Amine Aux.	MW$_{el}$	1.6	1.4	–	–
Syngas Compressors	MW$_{el}$	32.3	26.7	30.8	26.2
Refrigeration Compressors	MW$_{el}$	10.9	10.2	11.4	10.2
Fuel Compressors	MW$_{el}$	0.7	–	19.2	–
Pumps	MW$_{el}$	1.6	1.0	0.9	0.5
Heat Rejection	MW$_{el}$	1.6	1.0	1.0	0.8
Generators					
Steam Turbine	MW$_{el}$	62.2	50.1	22.5	35.4
NH_3 Expander	MW$_{el}$	1.1	1.4	1.1	1.2
Gas Turbine	MW$_{el}$	24.1	–	–	
N_2 Turbine	MW$_{el}$	–	–	6.8	
Total Auxiliaries	MW$_{el}$	88.8	74.2	102.6	55.6
Net Power	MW$_{el}$	−1.4	−22.7	−72.2	−19.0

The green NH_3 plant produces pure hydrogen at 30 bar via electrolysis at an efficiency of 70% (LHV). This is considerably lower than the hydrogen production efficiencies of the blue NH_3 plants, which also leads to a lower NH_3 production efficiency and a higher specific energy consumption. In addition to the electrolyser power consumption, a moderate amount of auxiliary consumption is also required because the compressors in the NH_3 synthesis loop and cryogenic N_2 separation power demand exceed the power produced by the steam turbine, further reducing the equivalent NH_3 production efficiency. Comparing the hydrogen and ammonia production efficiencies in this way equates the primary energy input of intermittent wind and solar electricity in green plants to the primary energy input of natural gas in blue plants. For blue plants, electricity input is valued more highly in the calculation of the equivalent natural gas input (Eq. (5)) because a steady supply of electricity is required. Finally, it is noted that the use of intermittent wind and solar power will require additional auxiliary consumption for energy storage, dependent on the amount and type of energy storage needed. This additional power consumption is not considered in Table 6, but it is accounted for in the optimization model used to find the minimum levelized cost of green NH_3.

In terms of CO_2 emissions, it can be seen that the LAC concept can only capture 76.3% of the CO_2 produced. Emissions arise from unconverted methane in the primary reformer, CO slip from the isothermal shift and imperfect CO_2 capture in the absorption unit. The KBR concept accomplishes a higher degree of capture by 6.5%-points, in virtue of the higher conversion of CH_4 and CO taking place in the FTR and ATR, and the conventional WGS train respectively. Finally, the GSR based concept reaches a CO_2 capture of 94.4%, with emissions originating mainly from undesired mixing in the cluster outlet stream, which are vented during the purification of the main N_2 stream, and the vent from the CPU unit. In terms of specific emissions (CO_2 per ton of ammonia), the GSR based concepts clearly outperform the reference benchmarks due to higher degree of capture and lower natural gas feed requirements for the nominal production. The green NH_3 plant involves no CO_2 emissions.

3.2. Economic results

Economic results are presented in three sections. First, the base case results for the blue NH_3 plants are shown with a decomposition of the capital cost, operating costs and levelized product cost for each plant. Secondly, sensitivity analysis to key economic parameters affecting the blue NH_3 plants is described. Finally, the blue ammonia plants are compared with green ammonia production using wind and solar resources available at different locations (Germany, Spain, and Saudi Arabia).

3.2.1. Blue NH_3 base cases

Fig. 4 shows the specific total overnight costs for each plant in k€/tpd of NH_3. Overall, the LAC plant shows 12 k€/tpd (-4.1%) lower costs than the KBR plant, while the GSR design offers a 71.9 k€/tpd (-24.8%) specific cost reduction. Notably, the reformer island of the LAC process is 20.2 k€/tpd (-30.6%) lower than the KBR, although this cost reduction is cancelled by the additional cost of the N_2 production unit. The GSR island costs about the same as the LAC reformer, but it avoids the costs of the CO_2 absorber and the N_2 production unit due to the inherent separation of CO_2 and N_2 in the GSR reduction and oxidation steps. The KBR plant presents the larger costs in units downstream the reformer due to the higher volumetric flow rate resulting from N_2 addition in the ATR.

On the other hand, the synthesis loop, refrigeration, and storage units represent 38.2% and 38.5% of the TOC of the KBR and LAC plants respectively, while these sections constitute up to 46.0% of the cost for the GSR design. The significant cost reductions of the GSR plant are achieved primarily through the avoidance of the MDEA unit, a cheaper reformer, steam cycle and CO_2 compression units, despite the larger costs of the PSA unit, which includes a syngas booster compressor.

The operating costs in €/ton of NH_3 are presented in Fig. 5. As expected, the costs of natural gas for the GSR plant are 36.4 €/ton (-24.5%) lower than for the KBR plant, while only 11.6 €/ton (-6.3%) less for the LAC. However, when also accounting for electricity costs, the total energy costs of all three plants are similar. The substantial GSR cost shift from natural gas to electricity illustrates how the GSR concept can achieve partial electrification of ammonia production. The CO_2 tax, transport and storage contribution is 22.3 €/ton (-40.8%) lower for the GSR plant relative to KBR, while the LAC presents 4.7 €/ton (8.5%) higher costs for this item. This are a direct consequence of a) the CO_2 capture performance (needed to avoid the CO_2 tax of 100 €/ton) and b) the required fuel input to each plant (influencing the total CO_2 production).

The levelized cost of ammonia (LCOA) of the different configurations is presented in Fig. 6; further details be found in the associated SEA tool files [54]. For the KBR design, a separate evaluation is made considering no CCS, to highlight that the CO_2 avoidance cost (for the assumed CO_2 tax) is negative for all plants which do incorporate CCS. Specifically, the KBR process without CCS leads to specific emissions of 1.62 kg of CO_2/
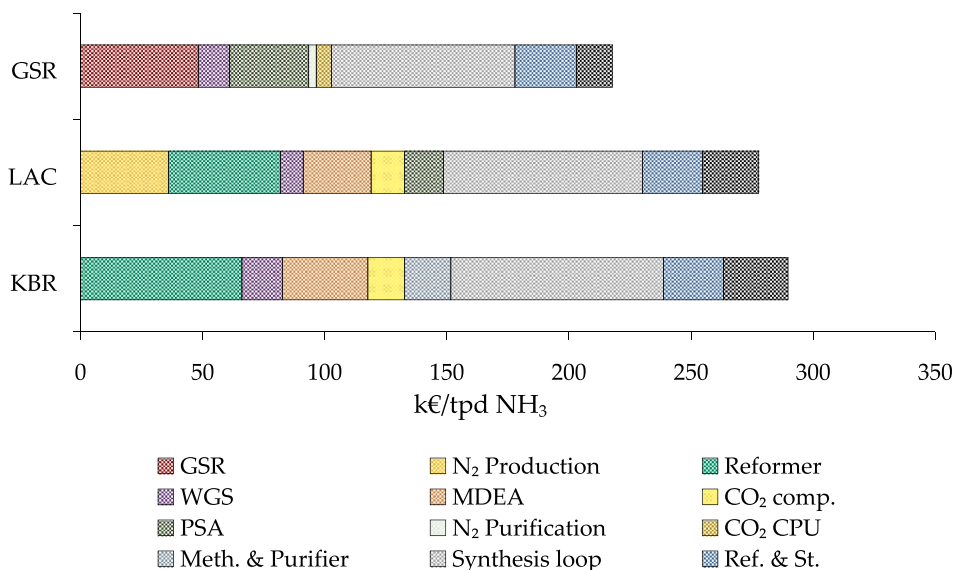

Fig. 4. Specific capital costs, i.e., ratio between total overnight costs and plant capacity, in k€/tpd for the different NH_3 plants.
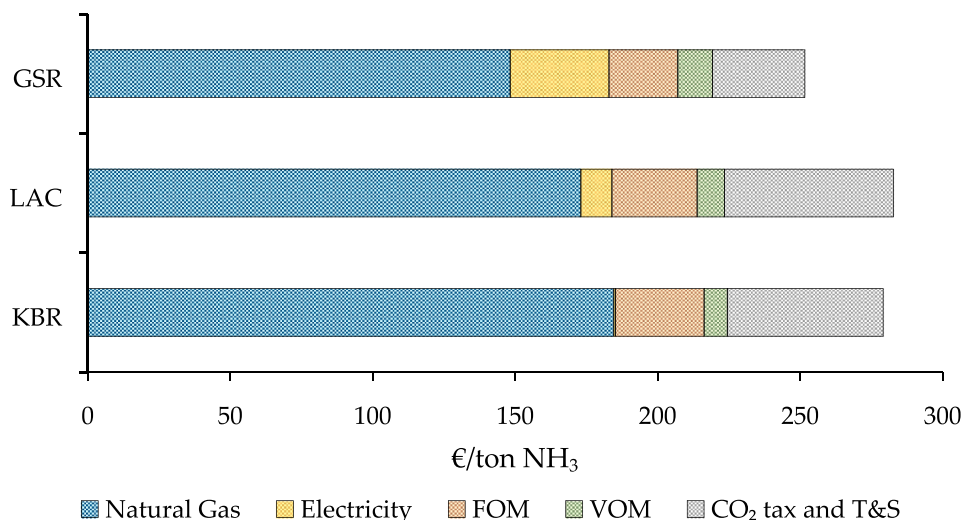
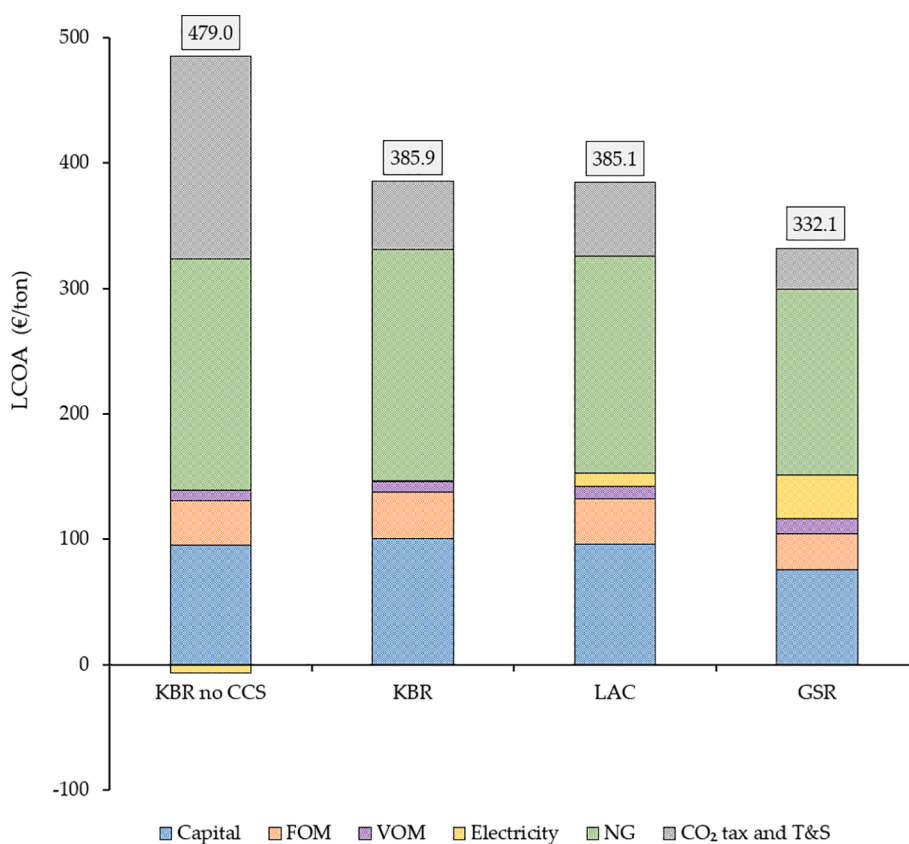**Fig. 5.** Specific operating costs for the different NH₃ plants.

Fig. 6. LCOA of the different blue NH₃ plants. (For interpretation of the references to colour in this figure legend, the reader is referred to the web version of this article.)

kg of NH₃, presenting an LCOA which is 93.1 €/ton higher (24.1%). The small capital cost reduction and revenues from electricity sales of the unabated plant are far smaller than the added costs from the carbon tax (at 100€/ton). On the other hand, the LAC plant presents practically the same levelized cost as the KBR design, showing larger contributions for CO₂ tax (due to the lower capture performance) and electricity imports, while the capital costs and fuel inputs are reduced. Finally, the GSR plant yields a LCOA which is 53.8 €/ton (-13.9%) lower than the KBR plant. Significant cost reductions are observed for items such as CO₂ tax,

storage and transportation, natural gas, and capital costs, despite the notable increase in the cost component of electricity imports.

3.2.2. Blue NH₃ sensitivity analysis

Sensitivity analyses illustrating the effect of key economic assumptions on the LCOA of blue NH₃ technologies are presented in Fig. 7. Natural gas price has the largest impact on the LCOA from all the variables considered, the effect being larger for the two reference plants presenting a higher consumption per ton of NH₃. CO₂ tax is the next
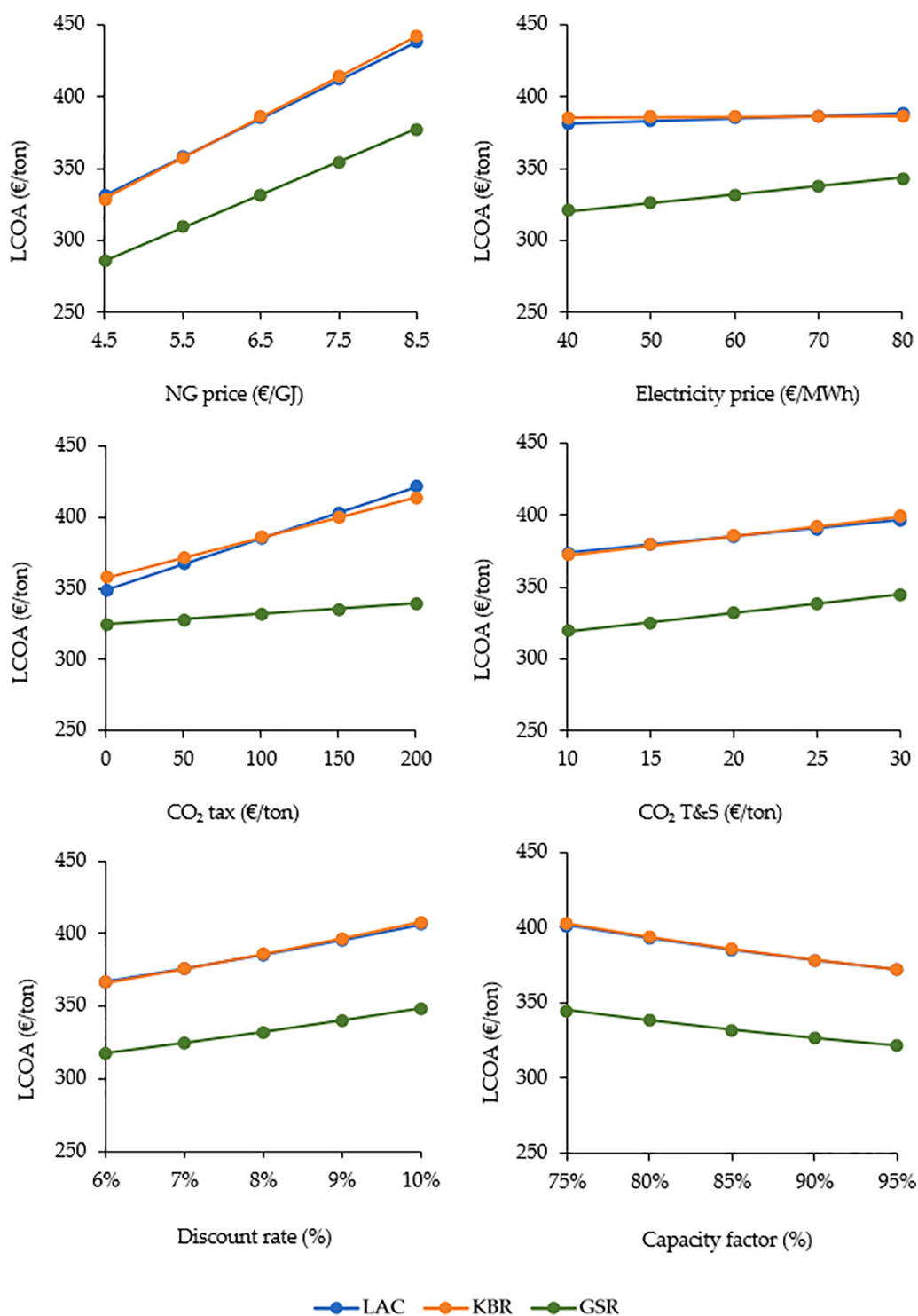
Fig. 7. Sensitivity analysis for the different blue NH$_3$ plants. (For interpretation of the references to colour in this figure legend, the reader is referred to the web version of this article.)

most influential variable, with a greater steepness for the benchmark processes as a result of attaining lower capture rates, compared to the GSR concept. Notably, it should be mentioned that even at no CO$_2$ tax, the GSR plant prevails in terms of economic attractiveness with respect to both benchmarks, while the LAC configuration becomes slightly more economical than the KBR plant in this scenario because it is no longer penalized for its higher CO$_2$ emissions intensity. The cost of transportation and storage shows similar effect in the cost of product for all the plants.

As expected, the influence of the electricity price is most prominent for the GSR plant, which requires significant power imports, although it remains significantly more competitive than the benchmark plants even for the highest power cost considered. Thus, the GSR concept presents the opportunity for partial electrification of ammonia production. This feature could be further exploited if heat is supplied to the reforming step of the reactors through optional ohmic heating of the steel metal rods used to provide thermal mass at times when cheap electricity is available, promoting fuel efficiency enhancements and potential

economic benefits. Furthermore, the GSR plant is least sensitive to changes in the discount rate and plant capacity factor because of its lower capital costs.

Finally, it should be stated that a large variation (+-100%) of nickel oxygen carrier cost presented a very small impact in the LCOA of the GSR concept, and is not shown in the figure above. Therefore, a shorter oxygen carrier lifetime will not critically affect the feasibility of the concept which, together with the conservative assumption for maximum operating GSR temperature, further increases the robustness of the design, critical for a successful long-term deployment. Thus, it can be safely concluded that the GSR concept will remain more economically attractive than the benchmark KBR and LAC technologies under any foreseeable market scenario.

3.2.3. Benchmarking against green NH₃

The blue NH$_3$ plants evaluated in this work were compared to green NH$_3$ plants under consistent assumptions for the year 2050, using the system optimization model detailed in the Supplementary Material. Detailed datafile for all cases as well as the GAMS model are available online [59]. The optimal capital deployment for the green NH$_3$ plants built in the three regions considered is shown in Fig. 8.

When comparing the renewable electricity generation in the three regions, Germany and Spain rely on wind and solar power, whereas the optimal mix is 100% solar PV in Saudi Arabia. The combination of wind and solar power gives German electricity production an overall higher capacity factor with lower peak production, allowing for a smaller electrolyser capacity. Also, the reliance on wind energy in Germany causes temporal variations over longer timescales, making it more economical to rely heavily on NH$_3$ storage and less on H$_2$ storage, thus requiring a larger ammonia production capacity to handle a larger peak hydrogen input.

When looking at the storage deployment in Fig. 8, Germany and Spain deploy no battery storage because of the longer timescales of wind variability. Due to the more regular daily production pattern of solar, Saudi Arabia deploys a small amount of battery storage which is combined with hydrogen storage to supply a near-steady hydrogen stream to the ammonia synthesis plant which operates at a capacity factor of 94%. Despite relying on solar for 84% of its generation, Spain needs to deploy more than 2.5x larger ammonia storage capacity than Saudi Arabia because it is located further from the equator, resulting in significant

seasonal variations in solar power output.

The optimized green ammonia costs are compared with the blue ammonia plants in Fig. 9. In Europe, green NH$_3$ is much cheaper by 202.8 €/ton (-26.3%) in Spain than Germany due to the much higher quality solar resource. The input electricity for Spanish green NH$_3$ is half the cost of Germany, but the higher electrolyser and hydrogen storage capacity required to utilize most of the produced solar power cancels out some of these gains. However, Spanish green NH$_3$ is 184.1 €/ton (+47.8%) more expensive than blue NH$_3$ produced with the LAC process and 237.2 €/ton (+71.4%) more expensive than the GSR process. Saudi Arabian green NH$_3$ is even cheaper than Spanish Green NH$_3$ by 84.5 €/ton (-17.4%), but the much lower natural gas costs in Saudi Arabia also cause drastic reductions in blue NH$_3$ costs. Overall, green NH$_3$ in Saudi Arabia is 246.1 €/ton (+103.1%) more expensive than blue NH$_3$ using the LAC process and 292.0 €/ton (+151.5%) more expensive than the GSR process.

It should also be pointed out that the green NH$_3$ costs shown in Fig. 9 may be mildly optimistic for three reasons: 1) the optimization is done over only one year of wind and solar variability, 2) perfect foresight regarding wind and solar power generation over the whole year is assumed, and 3) all equipment is assumed to have 100% availability (relative to an 85% capacity factor for the blue technologies). In practice, these factors would require various parts of the plant to be over-sized relative to the perfectly optimized values calculated in the model.

Given the inherent uncertainty of projecting technology costs to 2050, the sensitivity of the green NH$_3$ plants to changes in the costs of wind & solar power and electrolysers is shown in Fig. 10. Significant uncertainty is also involved in the operating flexibility of the NH$_3$ loop, so a sensitivity assessment to the minimum operating load is also conducted. The sensitivity to the ramp rate assumption of 20%/hour was also checked, but even a very low ramp rate of 1%/hour only increased the LCOA by about 1%. This low sensitivity to the ramp rate results because flexible operation of the NH$_3$ loop is used mainly for balancing long-term variations in wind and solar output and slow ramp rates can be economically counterbalanced by shorter-term hydrogen storage. The optimization was redone in each case to allow the model to change the deployment ratios of equipment in response to the cost variations in selected components.

As shown in Fig. 10, the green NH$_3$ pathways remain considerably more expensive than the GSR blue NH$_3$ pathway even at low green
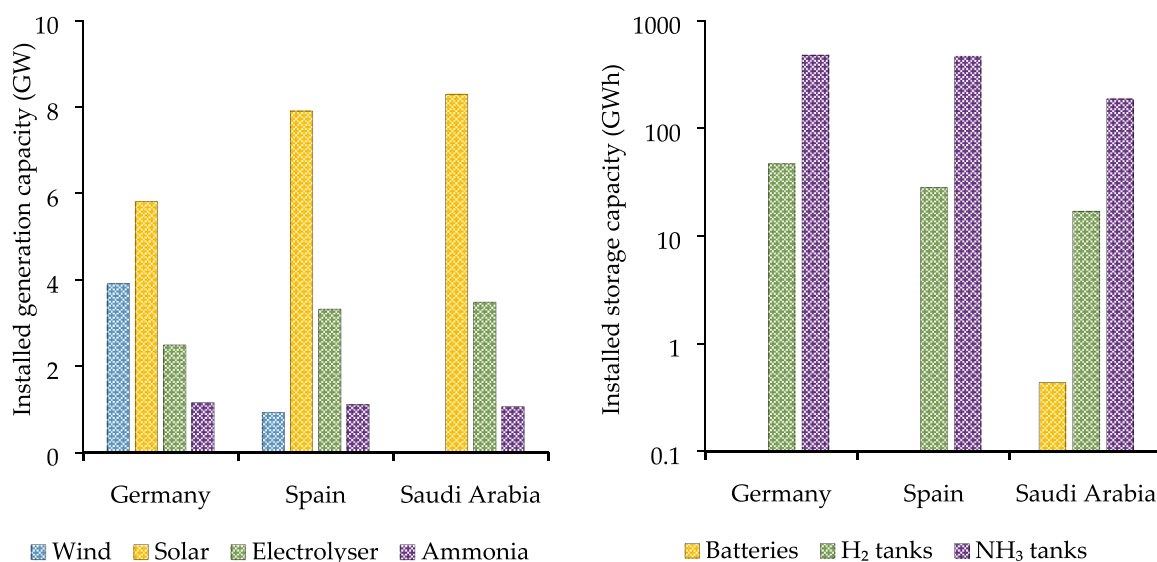

Fig. 8. Optimal generation and storage capital deployment in the 1 GW green NH$_3$ plants located in three regions. Note that the storage graph is plotted on a logarithmic axis due to the large differences in deployment. (For interpretation of the references to colour in this figure legend, the reader is referred to the web version of this article.)
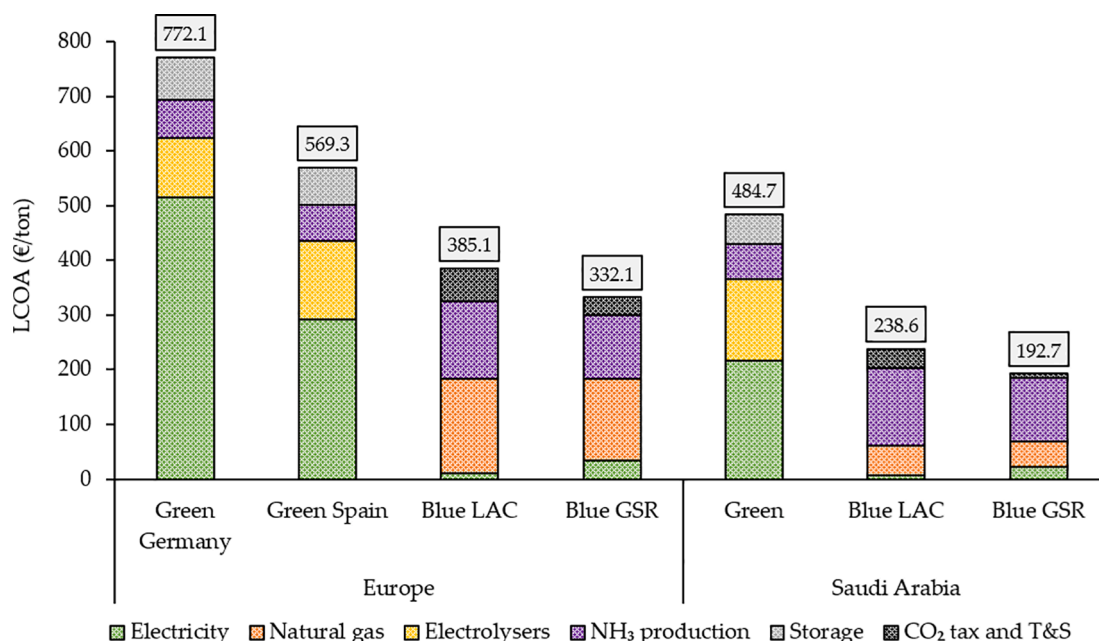
Fig. 9. Comparison of blue and green ammonia production in Europe and Saudi Arabia by mid-century. (For interpretation of the references to colour in this figure legend, the reader is referred to the web version of this article.)

technology costs. German green NH_3 is most sensitive to wind costs because of its low-quality solar resource, whereas the opposite is true in Spain and Saudi Arabia, leading to a higher dependency on solar PV costs. Electrolyzer sensitivity is somewhat lower in Germany because of the higher combined capacity factor of its balanced mix of wind and solar generation that results in a lower electrolyzer capacity requirement (Fig. 8). Increasing the minimum achievable load of the NH_3 loop substantially increases the LCOA in Germany and Spain because these regions require flexibility in NH_3 production for the balancing of seasonal variations and long-term fluctuations in wind output. However, decreasing the minimum achievable load below 50% had only a minor benefit because the efficiency losses resulting from large output reductions (see Supplementary Material) impose considerable additional costs on the system, causing the model to exploit the full range of operation only on rare occasions. Solar production in Saudi Arabia is highly reliable throughout the year, so it is minimally affected by NH_3 production loop flexibility.

Spanish green NH_3 gets closest to its blue benchmark (European blue NH_3). If wind, solar, and electrolyser costs are simultaneously reduced by 30% and the minimum achievable load of the NH_3 loop is set to 20%, the Spanish LCOA falls to 429 €/ton, which is 29% higher than the GSR process. In other words, the natural gas price would have to rise from 6.5 to 10.7 €/GJ for the most optimistic green NH_3 scenario to outcompete the GSR technology in Spain. For perspective, the highest European natural gas price projected by the IEA [1] for 2050 is 8.0 €/GJ in the Stated Policies Scenario that predicts 27% growth in global natural gas consumption and results in 2.6 °C of global temperature rise by 2100. If a massive green policy push drives down the costs of wind, solar, and electrolysers to the lower bounds explored in Fig. 10, natural gas prices are more likely to be around 4.3 €/GJ as projected for the IEA Sustainable Development Scenario, reducing the LCOA of GSR to 282 €/GJ (34% below the optimistic green NH_3 benchmark). Thus, the conclusion that long-term blue NH_3 will remain substantially cheaper than its green counterpart is robust.

Finally, an interesting observation can be made regarding the low LCOA in Saudi Arabia: Blue NH_3 can compete with liquified natural gas (LNG) in a future low-carbon world. Specifically, NH_3 production with GSR in Saudi Arabia would cost 10.4 €/GJ (Fig. 9) compared to around 7.0 €/GJ for LNG based on IEA estimates [60]. If the blue NH_3 plant

would be built on the enormous scale of typical LNG facilities, its levelized capital cost would further reduce. It is also likely that Middle Eastern plants would be cheaper than the European costs used in this assessment. For example, a 40% reduction in capital costs would bring blue NH_3 costs down to 7.9 €/GJ. Under the assumption that international shipping costs are small and similar (NH_3 is cheaper to store but less energy dense than LNG), this means that a CO_2 tax at the point of use of only 20 €/ton would render NH_3 more economical than LNG, even when ignoring any CO_2 and methane emissions during LNG production and distribution.

4. Summary & conclusions

This study evaluates from a techno-economic perspective the performance of several ammonia production plants using natural gas and/or electricity as feedstock. Two reference plants using existing technologies were assessed as benchmarks: the Kellogg-Braun and Root (KBR) Purifier process and the Linde Ammonia Concept (LAC). These reference plants create a basis of comparison for two future-oriented NH_3 production plants: a gas switching reforming (GSR) plant design producing blue NH_3 (natural gas fuel with CO_2 capture) and an electrolytic green NH_3 production facility (including electricity, hydrogen, and ammonia storage to account for variability of wind and solar power) in three different world regions. The main conclusions drawn from the study are summarized as follows:

- The KBR plant yielded an equivalent specific fuel consumption of 28.5 GJ/ton of NH_3, with a CO_2 capture rate of 82.8% and specific emissions of 0.28 ton/ton, whereas the LAC plant presented a higher efficiency of 27.7 GJ/ton, at the cost of a lower a CO_2 capture ratio of 76.3% and higher specific emissions of 0.36 ton/ton. The GSR concept achieved an even lower equivalent energy consumption of 26.2 GJ/ton (13% of which represents electricity imports), while capturing 94.4% of the CO_2 produced resulting in minimal specific emissions of 0.07 ton/ton. Green NH_3 required 31 GJ of electrical energy per ton of NH_3 with no CO_2 emissions.
- From an economic perspective, the KBR process achieves a levelized cost of ammonia (LCOA) of 385.9 €/ton. When the plant is designed without CCS, the cost rises to 479.0 €/ton (19.4% increase) at a CO_2
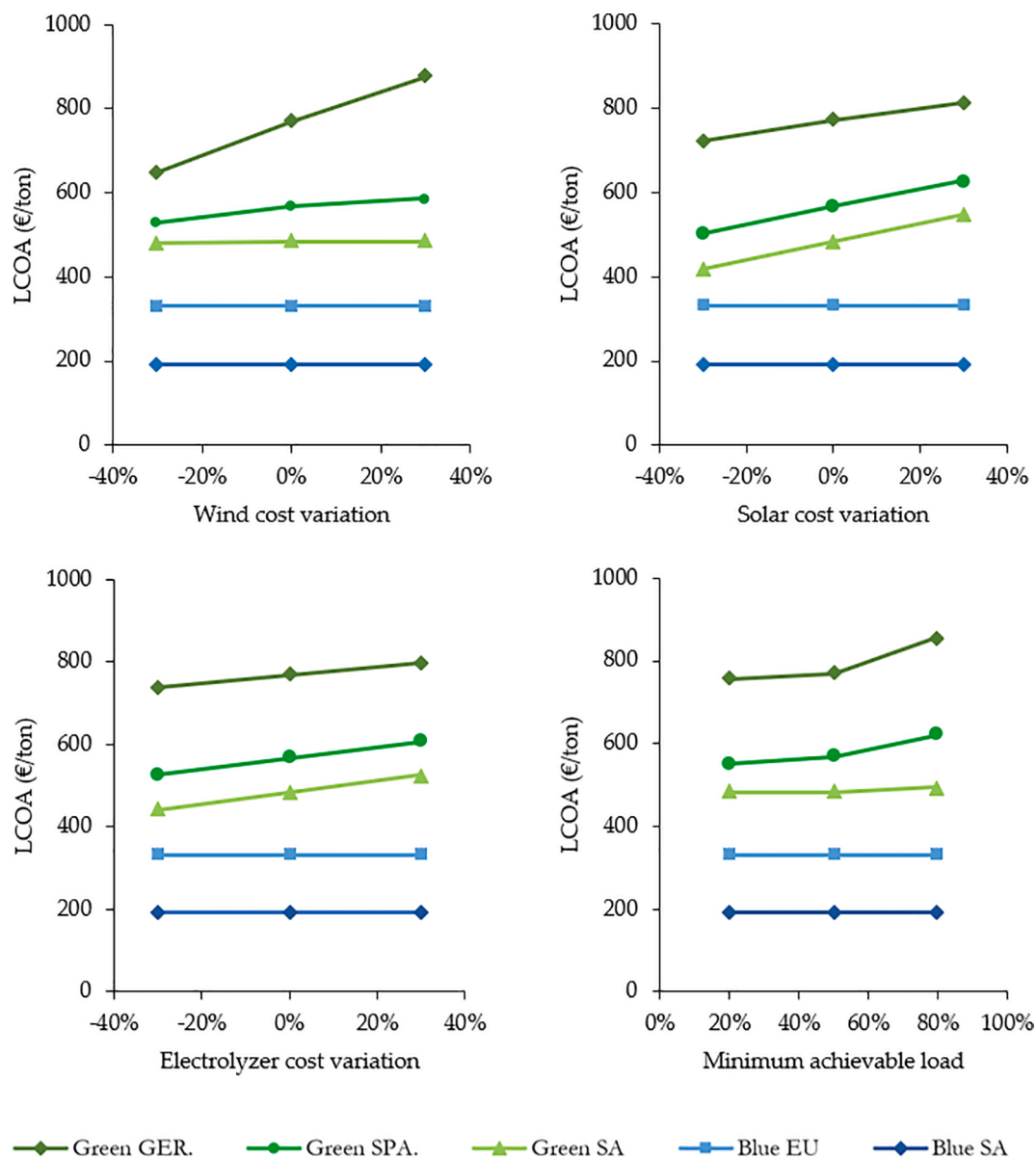
Fig. 10. Sensitivity of long-term green hydrogen competitiveness to costs of wind turbines, solar panels, and electrolysers as well as the minimum achievable load in the NH_3 loop. Blue NH_3 is represented by the GSR technology in this mid-century comparison. Central values for wind, solar, and electrolyser costs are 1117 €/kW, 317 €/kW, and 512 €/kW_{H2}, respectively. (For interpretation of the references to colour in this figure legend, the reader is referred to the web version of this article.)

tax of 100 €/ton. The LAC plant reaches an almost identical LCOA as the KBR (385.1 €/ton), while for the GSR concept the cost falls to 332.1 €/ton (-13.9%). Variations in natural gas price and CO_2 tax presented the largest effect on the LCOA.

- Using cost assumptions applicable to 2050, fully optimized green ammonia production from wind and solar power with electrolysers and energy storage showed substantially higher costs than the blue NH_3 alternatives: 772.1, 569.3, and 484.7 €/ton in Northern Germany, Southern Spain, and Saudi Arabia, respectively. Moreover, the LCOA of blue NH_3 production in Saudi Arabia reduced to 192.7 €/ton with the GSR process due to much lower energy costs.

In view of the techno-economic results attained in this study, there is a strong case for further research and development of the GSR process for blue ammonia production. The inherent CO_2 capture achieved by GSR makes it fundamentally more attractive as a low-carbon hydrogen production technology than conventional steam methane reforming, while additional benefits are derived for NH_3 synthesis from the co-

production of a high-purity pressurized N_2 stream. Furthermore, the GSR concept presents an opportunity to partially electrify the ammonia production process through optional ohmic heating during the reforming step at times when cheap renewable electricity is available.

In conclusion, ammonia has great potential to become a carbon-free energy vector in the future, since the industrial synthesis of this commodity is well-known and it is easy and cheap to transport and store, with a highly developed pre-existing infrastructure. This work shows that advanced blue NH_3 processes like GSR can achieve considerable cost reductions relative to conventional process routes and that these plants will remain more competitive than green ammonia production through water electrolysis employing renewable power in the long-term future. The cost of both green and blue NH_3 is highly sensitive to location and, given that ammonia is relatively simple to transport and store, production should be concentrated in regions with the cheapest input energy. Blue NH_3 may present a cost competitive export energy vector alternative to LNG, even at mild CO_2 pricing. The timely commercialization of advanced blue NH_3 concepts like GSR therefore emerges as a

high priority for natural gas exporting regions as the global decarbonization effort continues to gather momentum.

CRediT authorship contribution statement

Carlos Arnaiz del Pozo: Conceptualization, Methodology, Formal analysis, Investigation, Writing – original draft. **Schalk Cloete:** Conceptualization, Methodology, Formal analysis, Investigation, Writing – original draft, Writing – review & editing, Funding acquisition.

Declaration of Competing Interest

The authors declare that they have no known competing financial interests or personal relationships that could have appeared to influence the work reported in this paper.

Acknowledgements

Appendix A. Supplementary data

Supplementary data to this article can be found online at https://doi.org/10.1016/j.enconman.2022.115312.

References

[1] [1] IEA, "World Energy Outlook. 2021, International Energy Agency." 2021.
[2] IEA "Global Hydrogen Review 2021, International Energy Agency 2021 Paris".
[3] IEA, "The future of hydrogen: Seizing today's opportunities. International Energy Agency: Paris" 2019.
[4] Cloete S, Ruhnau O, Hirth L. On capital utilization in the hydrogen economy: The quest to minimize idle capacity in renewables-rich energy systems. Int J Hydrogen Energy 2020.
[5] Kovač A, Paranos M, Marciuš D. Hydrogen in energy transition: A review. Int J Hydrogen Energy 2021.
[6] Nazir H, Muthuswamy N, Louis C, Jose S, Prakash J, Buan ME, Flox C, Chavan S, Shi X, Kauranen P. Is the H2 economy realizable in the foreseeable future? Part II: H2 storage, transportation, and distribution. Int J Hydrogen Energy. 2020;45(41):20693–708.
[7] Wang Z, Wang Y, Afshan S, Hjalmarsson J. A review of metallic tanks for H2 storage with a view to application in future green shipping. Int J Hydrogen Energy. 2021;46(9):6151–79.
[8] Bartels JR, "A feasibility study of implementing an Ammonia Economy", 2008.
[9] Elishav O, Mosevitzky Lis B, Valera-Medina A, Grader GS. "Chapter 5 - Storage and Distribution of Ammonia" 2021, pp. 85-103.
[10] Hånde R, Wilhelmsen Ø. Minimum entropy generation in a heat exchanger in the cryogenic part of the hydrogen liquefaction process: On the validity of equipartition and disappearance of the highway. Int J Hydrogen Energy. 2019;44(29):15045–55.
[11] Hammad A, Dincer I. Analysis and assessment of an advanced hydrogen liquefaction system. Int J Hydrogen Energy. 2018;43(2):1139–51.
[12] Lim J, Fernández CA, Lee SW, Hatzell MC. Ammonia and Nitric Acid Demands for Fertilizer Use in 2050. ACS Energy Lett 2021;6:3676–85.
[13] Ezzat MF, Dincer I. Energy and exergy analyses of a novel ammonia combined power plant operating with gas turbine and solid oxide fuel cell systems. Energy. 2020;194.
[14] Hansson J, Fridell E, Brynolf S. "On the potential of ammonia as fuel for shipping: a synthesis of knowledge" 2020.
[15] Cechetto V, Di Felice L, Medrano JA, Makhloufi C, Zuniga J, Gallucci F. H2 production via ammonia decomposition in a catalytic membrane reactor. Fuel Process Technol. 2021;216.
[16] Rouwenhorst KHR, der Ham Van, Aloijsius GJ, Mul G, Kersten SRA. Islanded ammonia power systems: Technology review & conceptual process design. Renew Sustain Energy Rev 2019;114.
[17] Cloete S, Khan MN, Nazir SM, Amini S. Cost-effective clean ammonia production using membrane-assisted autothermal reforming. Chem Eng J 2021;404.
[18] Lee Pereira RJ, Argyris PA, Spallina V. A comparative study on clean ammonia production using chemical looping based technology. Appl. Energy. 2020;280.
[19] Martínez I, Armaroli D, Gazzani M, Romano MC. Integration of the Ca–Cu Process in Ammonia Production Plants. Ind Eng Chem Res. 2017;56(9):2526–39.
[20] Rydén M, Lyngfelt A, Mattisson T. Synthesis gas generation by chemical-looping reforming in a continuously operating laboratory reactor. Fuel 2006;85(12–13):1631–41.
[21] Ishida M, Zheng D, Akehata T. Evaluation of a chemical-looping-combustion power-generation system by graphic exergy analysis. Energy 1987;12:147–54.
[22] Mattisson T, Keller M, Linderholm C, Moldenhauer P, Rydén M, Leion H, Lyngfelt A. Chemical-looping technologies using circulating fluidized bed systems: Status of development. Fuel Process Technol. 2018;172:1–12.
[23] Zaabout A, Cloete S, Johansen ST, Van SA, Gallucci F, Amini S. Experimental demonstration of a novel gas switching combustion reactor for power production with integrated CO 2 capture. Ind Eng Chem Res 2013;52(39):14241–50.
[24] Spallina V, Marinello B, Gallucci F, Romano MC, Van Sint Annaland M. Chemical looping reforming in packed-bed reactors: Modelling, experimental validation and large-scale reactor design. Fuel Process Technol 2017;156:156–70.
[25] Wassie SA, Gallucci F, Zaabout A, Cloete S, Amini S, van Sint Annaland M. Hydrogen production with integrated CO2 capture in a novel gas switching reforming reactor: Proof-of-concept. Int J Hydrogen Energy. 2017;42(21):14367–79.
[26] Zhang H, Wang L, Van herle J, Maréchal F, Desideri U. Techno-economic comparison of green ammonia production processes. Appl Energy 2020;259.
[27] Sánchez A, Martín M. Optimal renewable production of ammonia from water and air. J Clean Prod 2018;178:325–42.
[28] Ozturk M, Dincer I. An integrated system for ammonia production from renewable hydrogen: A case study. Int J Hydrogen Energy. 2021;46(8):5918–25.
[29] IRENA, "Renewable Power Generation Costs in 2020, International Renewable Energy Agency" 2021.
[30] IRENA, "Green hydrogen cost reduction: Scaling up electrolysers to meet the 1.5°C climate goal, International Renewable Energy Agency: Abu Dhabi" 2020.
[31] Osman O, Sgouridis S, Sleptchenko A. Scaling the production of renewable ammonia: A techno-economic optimization applied in regions with high insolation. J Clean Prod 2020;271.
[32] Wang L, Xia M, Wang H, Huang K, Qian C, Maravelias CT, Ozin GA. Greening ammonia toward the solar ammonia refinery. Joule 2018;2(6):1055–74.
[33] Morgan ER, Manwell JF, McGowan JG. Sustainable Ammonia Production from U.S. Offshore Wind Farms: A Techno-Economic Review. ACS Sustainable Chem Eng 2017;5(11):9554–67.
[34] Armijo J, Philibert C. Flexible production of green hydrogen and ammonia from variable solar and wind energy: Case study of Chile and Argentina. Int J Hydrogen Energy. 2020;45(3):1541–58.
[35] Gosnell J, Malhotra A. New Ammonia Process. Ammonia Plant Saf Relat Facil 2000;40:116–25.
[36] Pattabathula V, Richardson J. Introduction to ammonia production. CEP Magazine. 2016;2:69–75.
[37] https://www.linde-engineering.com/en/process-plants/hydrogen_and_synthesis_gas_plants/gas_products/ammonia/index.html 2021.
[38] Nayak-Luke R, Bañares-Alcántara R, Wilkinson I. "Green" Ammonia: Impact of Renewable Energy Intermittency on Plant Sizing and Levelized Cost of Ammonia. Ind Eng Chem Res. 2018;57(43):14607–16.
[39] Flórez-Orrego D, de Oliveira Junior S. Modeling and optimization of an industrial ammonia synthesis unit: An exergy approach. Energy. 2017;137:234–50.
[40] Lin B, Heng L, Fang B, Yin H, Ni J, Wang X, Lin J, Jiang L. Ammonia synthesis activity of alumina-supported ruthenium catalyst enhanced by alumina phase transformation. ACS Catal 2019;9(3):1635–44.
[41] Dyson DC, Simon JM. Kinetic Expression with Diffusion Correction for Ammonia Synthesis on Industrial Catalyst. Ind Eng Chem Fund 1968;7(4):605–10.
[42] Nazir SM, Cloete JH, Cloete S, Amini S. Pathways to low-cost clean hydrogen production with gas switching reforming. Int J Hydrogen Energy 2020.
[43] Nazir SM, Cloete JH, Cloete S, Amini S. Efficient hydrogen production with CO2 capture using gas switching reforming. Energy. 2019;185:372–85.
[44] Guo X, Vullum PE, Venvik HJ. "Inhibition of metal dusting corrosion on Fe-based alloy by combined near surface severe plastic deformation (NS-SPD) and thermochemical treatment" Corros. Corros Sci 2021;190.
[45] Holland ML, De Bruyn HJ. Metal dusting failures in methane reforming plant. Int J Pressure Vessels Piping 1996;66(1):125–33.
[46] Rege SU, Yang RT, Buzanowski MA. Sorbents for air prepurification in air separation. Chem Eng Sci 2000;55(21):4827–38.
[47] Spath PL, Dayton DC, "Preliminary screening–technical and economic assessment of synthesis gas to fuels and chemicals with emphasis on the potential for biomass-derived syngas" *Preliminary screening–technical and economic assessment of synthesis gas to fuels and chemicals with emphasis on the potential for biomass-derived syngas.* 2003.
[48] Kolster C, Mechleri E, Krevor S, Mac Dowell N. The role of CO2 purification and transport networks in carbon capture and storage cost reduction. Int J Greenhouse Gas Control 2017;58:127–41.
[49] Campanari S, Mastropasqua L, Gazzani M, Chiesa P, Romano MC. Predicting the ultimate potential of natural gas SOFC power cycles with CO2 capture – Part A: Methodology and reference cases. J Power Sources 2016;324:598–614.
[50] FCH. State of the art and future targets for fuel cell and hydrogen applications, https://www.fch.europa.eu/soa-and-targets [accessed on 02.11.2021].
[51] https://industry.airliquide.us/ammonia 2021.

[52] Carlos Arnaiz del Pozo, Schalk Cloete, and Ángel Jiménez Álvaro. Standard Economic Assessment (SEA) Tool. Available from: https://bit.ly/3hyF1TT.

[53] Carlos Arnaiz del Pozo, Schalk Cloete and Ángel Jiménez Álvaro. SEA Tool User Guide. Available from: https://bit.ly/3jq9Bkf.

[54] Arnaiz del Pozo C, Cloete S. "SEA Tool files: Blue-Green Ammonia. Available from: https://bit.ly/32PS92u 2021.

[55] Turton R, Bailie RC, W.B. Whiting and J.A. Shaeiwitz, "Analysis, synthesis and design of chemical processes", 2008.

[56] IEAGHG R&D Programme, "Effects of Plant Location on the Costs of CO2 Capture, Technical Report" 2018.

[57] Anantharaman R, Bolland O, Booth N, Van Dorst E, Sanchez Fernandez E, Franco F, Macchi E, Manzolini G, Nikolic D, Pfeffer A, Prins M, Rezvani S, Robinson L. "Cesar Deliverable D2.4.3. European Best Practice Guidelines For Assessment Of Co2 Capture Technologies" 2018.

[58] Pfenninger S, Staffell I. Long-term patterns of European PV output using 30 years of validated hourly reanalysis and satellite data. Energy. 2016;114:1251–65.

[59] Arnaiz del Pozo C, Cloete S. "GAMS model cases, Blue-Green Ammonia. Available from: https://bit.ly/3Hvicvt" 2021.

[60] IEA, "World Energy Outlook, International Energy Agency" 2018.